RSC Advances

COMMUNICATION

View Article Online
View Journal | View Issue

Cite this: *RSC Adv.*, 2016, **6**, 14134

Received 4th December 2015
Accepted 25th January 2016

DOI: 10.1039/c5ra25904e

www.rsc.org/advances

$[Re(CO)_3Cl(C_5H_4ClP)_2]$ and $[Re(CO)_2Cl(C_5H_4ClP)_3]$: synthesis and characterization of two novel rhenium(I) phosphinine complexes†

Manuela Hollering,[ab] Richard O. Reithmeier,[a] Simon Meister,[a] Eberhardt Herdtweck,[b] Fritz E. Kühn*[b] and Bernhard Rieger*[a]

Two novel rhenium(I) phosphinine complexes $[Re(CO)_3Cl(\eta^1\text{-}C_5H_4ClP)_2]$ (**1**) and $[Re(CO)_2Cl(\eta^1\text{-}C_5H_4ClP)_3]$ (**2**) were synthesized and the molecular structure of both was determined by single crystal X-ray diffraction. In compound **1** the two coordinated phosphinine ligands are arranged in a *cis* position, whereas compound **2** with three phosphinine ligands crystallizes in a *meridional* structural motif. Density functional theory investigations were executed to examine the relative stabilities of both complexes **1** and **2**.

Introduction

Heteroarenes of the type C_5H_5E (E = N, P, As, Sb, Bi) have found widespread interest and various applications over the years.[1–4] Particularly the ambidentate character of pyridines, phosphinines and their derivatives, which enables them to bind metals either *via* the heteroatom in η^1 or the π-system in η^6 coordination, helped to establish this versatile class of ligands in organometallic chemistry.[5–7] The synthesis of the first phosphinine derivative was described by Märkl in 1966.[8] However, only when Le Floch and Mathey reported more convenient synthetic methodologies, did functionalized phosphinines become more easily accessible.[9–11] Various coordination modes of phosphinines and their derivatives to numerous transition metals as well as their application in homogeneous catalysis have been reported since.[1–4,12–20] Recently, Mathey *et al.* and Amouri *et al.* have described copper and gold complexes featuring phosphinine derivatives with interesting structural motifs and possible catalytic and electronic utilization.[21,22] Although potential implementation of phosphinine transition metal complexes in homogeneous catalysis has been discussed in the literature, to the best of our knowledge, electron rich rhenium(I) complexes featuring η^1-coordinated phosphinines have not been reported in more detail, despite the scattered mentioning of such compounds.[4,6,23] The facile synthesis and characterization of two novel rhenium(I) complexes *cis*-$[Re(CO)_3Cl(\eta^1\text{-}C_5H_4ClP)_2]$ (**1**) and *mer*-$[Re(CO)_2Cl(\eta^1\text{-}C_5H_4ClP)_3]$ (**2**) are reported in this work.

Results and discussion

Reaction of $[Re(CO)_5Cl]$ with 2.5 eq. 2-chlorphosphinine in refluxing toluene results in a bright yellow solution, which upon removal of the solvent yields the crude product as a yellow solid. Subsequent crystallization from CH_2Cl_2/pentane leads to bright yellow crystals of **1** in quantitative yield (based on the Re precursor; Scheme 1).

Complex **1** was characterized by NMR and IR spectroscopy, elemental analysis and single crystal X-ray diffraction. **1** is soluble in chloroform, toluene and benzene, but insoluble in diethyl ether and *n*-pentane. In solution, only one set of resonances is observed at room temperature in ^1H, ^{13}C and ^{31}P spectra of **1**. ^{31}P spectrum shows a highfield shift of the phosphorus signal from 201.9 ppm (free ligand) to a broad signal at 169.4 ppm in **1**. ^{31}P–^{31}P coupling, which could confirm *cis* coordination of the ligands is not observed. A VT-NMR study revealed significant broadening of the signal at elevated temperatures, while a sharp singlet is obtained at lower temperatures.[24] Decoalescence is not

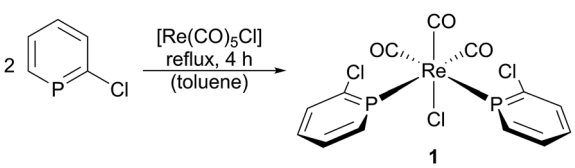

Scheme 1 Synthesis of complex **1**.

[a]*WACKER-Chair of Macromolecular Chemistry, Technische Universität München, Lichtenberg Straße 4, 85748 Garching b. München, Germany. E-mail: rieger@tum.de; Fax: +49-89-289-13562*

[b]*Chair of Inorganic Chemistry/Molecular Catalysis, Catalysis Research Center, Technische Universität München, Lichtenberg Straße 4, 85748 Garching b. München, Germany. E-mail: fritz.kuehn@ch.tum.de; Fax: +49-89-289-13473*

† Electronic supplementary information (ESI) available: NMR, UV/vis spectra of complexes **1** and **2** and computational and crystallographic details. CCDC 1005247 and 1005248. For ESI and crystallographic data in CIF or other electronic format see DOI: 10.1039/c5ra25904e

observed. This might be due to a fast dynamic equilibrium, since only one set of phosphinine signals is observed in ^{1}H, ^{13}C and ^{31}P NMR spectra. The molecular structure of **1** is shown in Fig. 1. The phosphinine ligands are arranged in *cis* position with *trans* positioned CO ligands in an overall distorted octahedral geometry. This arrangement explains the chemical equivalency of the two phosphinine rings in solution. Re–P bond lengths of 2.4154(13) and 2.4120(12) Å in compound **1** are similar, yet slightly shorter compared to Re–P bond lengths in the related complex *mer*-$[Re(CO)_3Cl(PEt_3)_2]$ with 2.430(1) Å.[25] Shorter bond lengths in compound **1** indicate – as previously mentioned[2] – π back-bonding character in electron rich transition metal complexes featuring phosphinine ligands.

The carbonyl vibrations in the IR spectra show a shift from ν_{CO} = 1983, 2046, 2155 cm^{-1} in the precursor $[Re(CO)_5Cl]$ to ν_{CO} = 1945, 1992, 2046 cm^{-1} in complex **1**, illustrating the σ-donating character of the phosphinine and the chlorido ligands.[25,26] The shift to lower wavenumbers in **1** is expected since carbonyls are known to be strong π-acceptors, while phosphinines act both as σ-donors and π-acceptors. The removal of two carbonyls during the formation of **1** additionally influences the remaining carbonyl shifts. In comparison to the related *mer*-$[Re(CO)_3Cl(PEt_3)_2]$ (ν_{CO} = 1887, 1940, 2045 cm^{-1}), the phosphinine ligands in **1** exhibit significantly lower σ-donor and higher π-acceptor capabilities than the triethylphosphine ligands.[25]

Further addition of 2-chlorphosphinine to compound **1** and subsequent refluxing in toluene leads to the formation of complex **2** as byproduct in yields up to 15% (based on complex **1**; Scheme 2).

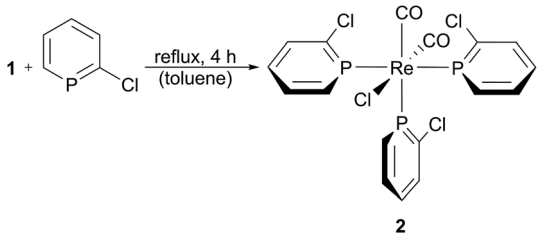

Scheme 2 Synthesis of complex **2**.

Complex **2** was characterized by NMR and IR spectroscopy, elemental analysis and single crystal X-ray diffraction. Solubility of **2** is analogous to **1**. Complexes **1** and **2** were separated *via* crystallization from CH_2Cl_2/*n*-pentane with complex **2** crystallizing as dark yellow crystals, similar to **1** in a distorted octahedral geometry (Fig. 2). The three η^1-coordinated phosphinines are arranged in a *meridional* structural motif, resulting in two phosphinines in *trans* position. This arrangement is to be expected, since 2-chlorphosphinine ligands are relatively bulky and the highest degree of freedom is presented in *mer*- rather than *fac*-coordination. In solution, two sets of signals are observed in ^{1}H, ^{13}C and ^{31}P spectra of **2**. Proximity of two sets of chemically not equivalent phosphorus heteroatoms results in a high multiplicity of resonances. The ^{31}P spectrum of compound **2** shows a less pronounced highfield shift of the phosphorus signals of the axial phosphinine (173.1 ppm) and of the two equatorial phosphinines (173.3 ppm), compared to the free 2-chlorphosphinine ligand (201.9 ppm) and to compound **1** (169.4 ppm). Both observed signals are broad, comparable to the situation observed for complex **1**. The signal at 173.3 ppm corresponds to a pseudo doublet with a $^{2}J_{P-P}$ coupling constant of 190 Hz for the *trans* standing phosphinines. *Cis* coupling was not observed for

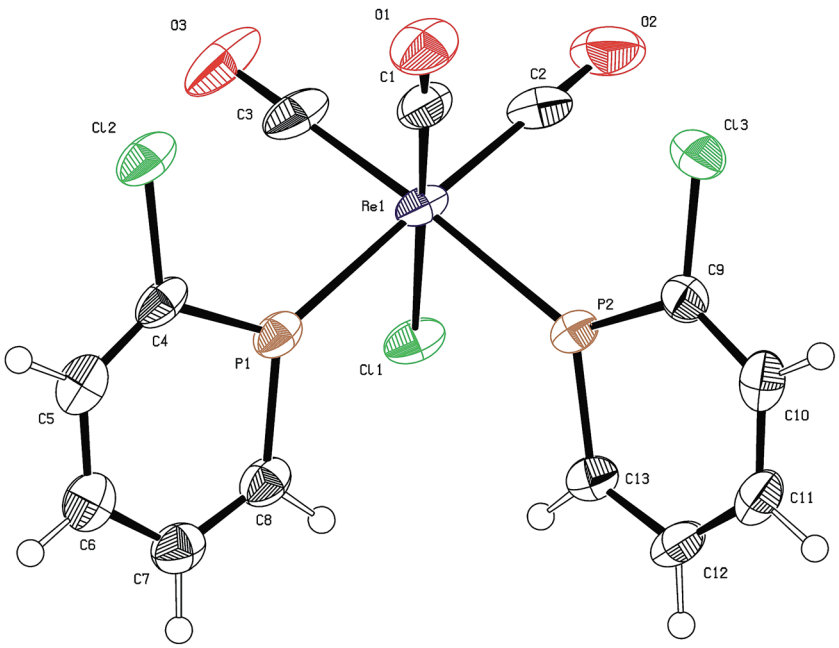

Fig. 1 ORTEP style drawing of **1**. Thermal ellipsoids are given at a 50% probability level. Selected bond lengths (Å) and angles (deg): Re1–P1, 2.4154(13); Re1–P2, 2.4120(12); Re1–Cl1, 2.4932(11); Re1–C1, 1.922(5); Re1–C2, 1.964(5); Re1–C3, 1.962(6); P1–Re1–P2, 89.66(4); Cl1–Re1–P1, 84.79(4); Cl1–Re1–P2, 85.42(4); P1–Re1–C3, 89.3(2); P2–Re1–C2, 89.74(14).

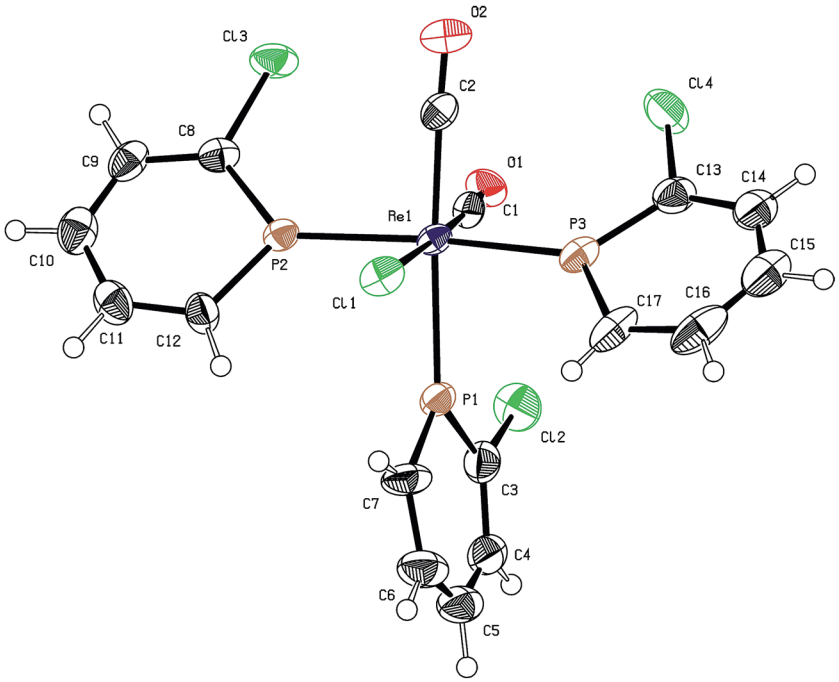

Fig. 2 ORTEP style drawing of **2**. Thermal ellipsoids are given at a 50% probability level. Selected bond lengths (Å) and angles (deg): Re1–P1, 2.4258(10); Re1–P2, 2.3584(13); Re1–P3, 2.3508(15); Re1–Cl1, 2.5162(14); Re1–C1, 1.919(5); Re1–C2, 1.950(4); P1–Re1–P2, 91.13(5); P1–Re1–P3, 86.16(5); P2–Re1–P3, 169.88(5); Cl1–Re1–P1, 85.00(4); Cl1–Re1–P2, 84.06(4); P1–Re1–C1, 95.51(16); P2–Re1–C2, 92.60(19).

either phosphinine ligand due to the broadness of the signals. The observed NMR data correspond well to the coordination geometry determined by single crystal X-ray diffraction.

Rhenium–phosphorus bond length Re–P1 of complex **2** differs considerably from the *trans*-positioned Re–P2 and Re–P3 bond lengths. The Re–P1 bond length with 2.4258(10) Å is similar, but slightly longer than the Re–P bond distances in complex **1**. The *trans*-arranged phosphinines in compound **2**, however, show shorter bond distances for Re–P2 (2.3584(13) Å) and Re–P3 (2.3508(15) Å) than previously reported bond distances.[25] Absence of a *trans*-positioned carbonyl ligand, which appears to be a stronger π-acceptor than phosphinine, possibly influences the bond distances due to relatively stronger π back-bonding for both phosphinines. These findings suggest strong σ-donor as well as π-acceptor character of the phosphinine ligands, which also has been noted before for other systems.[27–29]

The carbonyl vibrations in the IR spectra show a strong shift from ν_{CO} = 1983, 2046, 2155 cm^{-1} of the precursor $[Re(CO)_5Cl]$ to ν_{CO} = 1924, 1965 cm^{-1} of complex **2**, illustrating again the pronounced σ-donating character of the phosphinine and the chlorido ligand.[25,26] The shift from ν_{CO} = 1945, 1992, 2046 cm^{-1} of **1** to ν_{CO} = 1924, 1965 cm^{-1} of **2** further supports the more pronounced σ-donating character of phosphinine ligands compared to carbonyls, resulting in increased back-bonding of the metal center to the remaining carbonyl ligands. In comparison to the related *mer*-$Re(CO)_2Cl[P(OEt_3)]_3$ (ν_{CO} = 1969, 1980 cm^{-1}), the phosphinine ligands in **2** exhibit slightly higher σ-donor and lower π-acceptor abilities than the triethylphosphite ligands.[30] However, compared to *mer*-$Re(CO)_2Cl[PPh(OEt_2)]_3$ (ν_{CO} = 1873, 1985 cm^{-1}), the phosphinine ligands in **2** exhibit slightly lower σ-donor and higher π-acceptor capabilities than the phosphine ligands.[30] This difference indicates that phosphine ligands generally show π-bonding character, with phosphite ligands having a slightly more pronounced effect than phosphinine ligands.

DFT calculations

In order to gain more detailed information on complex **1** and **2** and π-acceptor properties of the 2-chlorphosphinine ligands, gas phase DFT calculations were carried out on a B3LYP/6-31+G** theory level. Detailed calculated bond lengths and angles can be found in the ESI† and correspond well to data obtained from the crystal structures. Calculated IR shifts correspond well to observed shifts.

In Fig. 3 calculated frontier orbitals of complex **1** are depicted. HOMO (Highest Occupied Molecular Orbital) as well as HOMO−1 of complex **1** are located mainly at the Re atoms, the carbonyl and chlorido ligands (Fig. 3, bottom). As mentioned before, complex **1** has a distorted octahedral geometry. The hardly overlapping HOMO and HOMO−1 are perpendicular to each other and have similar energy levels, HOMO −6.46 eV and HOMO−1 −6.47 eV, respectively. The calculated energy gap of only ΔE = 0.01 eV in the gas phase supports the experimental findings that both orbitals are degenerate in solution (the molecule has not been restricted to a certain point group).[31] LUMO (Lowest Unoccupied Molecular Orbital) and LUMO+1, on the other hand, are each located at one phosphinine ligand (Fig. 3, top). The LUMO at −2.48 eV and LUMO+1 at −2.45 eV are perpendicular to each other with very minor overlap. The energy gap of ΔE = 0.03 eV in the gas phase calculation implies a nearly degenerate character of both. Complex **1** has

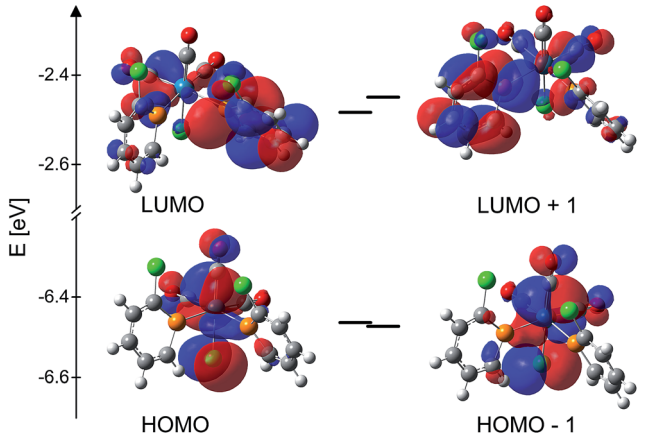

Fig. 3 Computed frontier orbitals of complex **1**. HOMO and HOMO−1 (bottom) and LUMO and LUMO+1 (top).

a calculated HOMO–LUMO gap of $\Delta E = 3.98$ eV, suggesting high kinetic stability.

Calculated frontier orbitals of complex **2** are depicted in Fig. 4. The HOMO of complex **2** (at −6.06 eV) is located mainly at the Re atom, the carbonyl and chlorido ligands (Fig. 4, bottom). HOMO−1 (at −6.13 eV) on the other hand, is 0.07 eV lower than the HOMO and is located not only on the Re atom, the carbonyl and chlorido ligands, but also partly on the phosphinine rings. The difference was to be expected, since the phosphinine ligands are chemically not equivalent, which is also evident from NMR spectra and single crystal X-ray diffraction. LUMO at −2.24 eV and LUMO+1 at −2.18 eV are located mainly at the phosphinine ligands (Fig. 4, top). The energy gap between the LUMOs of $\Delta E = 0.05$ eV is slightly smaller than the gap between the HOMOs of $\Delta E = 0.07$ eV. The higher energy difference in complex **2** between HOMO and HOMO−1 as well as LUMO and LUMO+1 originates from both differently shaped orbitals and location on different complex fragments, corresponding well with the solution-NMR spectra. The HOMO–LUMO gap of complex **2** ($\Delta E = 3.82$ eV) is slightly smaller than the gap in complex **1** ($\Delta E = 3.98$ eV), indicating slightly higher kinetic stability of **1**.

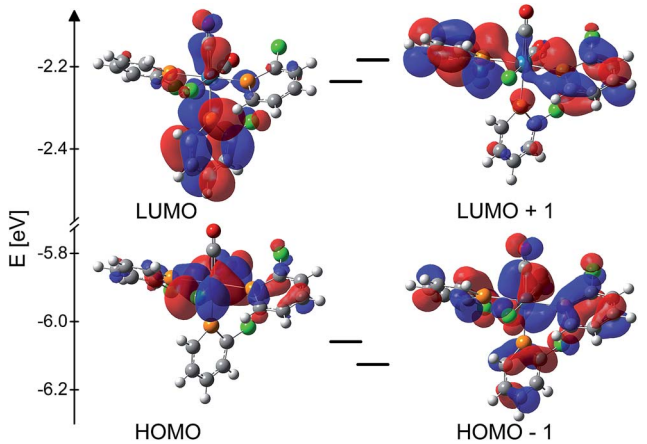

Fig. 4 Computed frontier orbitals of complex **2**. HOMO and HOMO−1 (bottom) and LUMO and LUMO+1 (top).

Natural bond order analysis is used to qualitatively estimate the character of the coordinative bonds and the resulting π-effects.[32–38] The relevant compositions of the orbitals are listed in Tables S1–S3† for the precursor $[Re(CO)_5Cl]$, **1** and **2**, respectively. The results show that in the precursor the strongest π back-bonding contribution of rhenium of 33% is directed toward the carbonyl ligand *trans* to chloride. This is to be expected, since chlorido ligands are effectively σ-donor ligands. It has to be noted, however, that even the Re–Cl bond shows π back-bonding character of 25% according to the calculations. The chemically equivalent four Re–C bonds in the plane show a calculated π back-bonding character of rhenium to carbon of 30% each. In **1** the highest contribution of rhenium of 33% is again directed to the carbonyl *trans* to chloride. However, the carbonyl ligands *trans* to the phosphinine ligands show a rather similar π back-bonding interaction at just below 33%. The Re–Cl bond has a calculated π back-bonding character of 23% in **1** and a rather high π back-bonding character of 28% for the Re–P bonds, indicating a stronger π-acceptor character of phosphinines compared to chloride, but a weaker π-acceptor character compared to carbonyl. Accordingly the strongest π back-bonding of 34% is calculated for the carbonyl *trans* to the chlorido ligand in complex **2**. The Re–P bond *trans* to carbonyl shows a slightly better back-bonding of 29% compared to complex **1**. However, the π back-bonding character of the Re–P bonds *trans* to each other is calculated to be 32% comparable to carbonyl ligands, confirming the π-acceptor character of phosphinines. The rhenium contribution to the Re–Cl π back-bonding is 23% in **2**. In case of rhenium, chloride and phosphor s, p and d orbitals are involved in the bond, in case of carbon only s and p orbitals contribute to the bond. The general trend of increased metal-to-ligand back-bonding is due to the step-wise removal of carbonyl ligands and addition of the σ-donor phosphinine, resulting in an overall higher electron density at the rhenium center.

Theoretical investigations on the two different coordination modes of complex **1** also support the higher thermodynamic stability of the *cis* configuration with a lower ground state free energy ΔG (12.9 kJ mol^{-1}) compared to the *trans* configuration. In case of complex **2** the *meridional* configuration has a lower ground state free energy ΔG (33.1 kJ mol^{-1}) compared to the *facial* configuration, which can be explained with steric hindrance of the bulky phosphorus heterocycles.

Conclusions

Reaction of $[Re(CO)_5Cl]$ with 2-chlorphosphinine in refluxing toluene leads to complex **1**. Subsequent addition of free ligand 2-chlorphosphinine to **1** and repeated refluxing in toluene leads to formation of complex **2**. To the best of our knowledge, complexes **1** and **2** are so far the first rhenium(I) phosphinine complexes with η^1-coordination. A combined analysis of NMR and IR spectroscopic data and single crystal X-ray data reveals both σ-donor and π-acceptor properties of the phosphinine ligand. The shape and energetic position of the highest

occupied and lowest unoccupied molecular orbitals of **1** and **2** gives information on relative stabilities. NBO analysis was carried out to better understand the π back-bonding situation in **1** and **2**.

Experimental

General comments

All reactions were performed under an atmosphere of dry argon in oven-dried glassware using standard Schlenk technique. All solvents were purified and dried by standard methods. Commercial available reagents were used without further purification. (Dichlormethyl)dichlorphosphine oxide,[39,40] (dichlormethyl) dichlorphosphine sulfide,[41] (dichlormethyl)dichlorphosphine[41,42] and 2-chlorphosphinine[9–11] were synthesized according to literature procedures. NMR spectra were obtained using Bruker AV360 and Bruker AV500 spectrometers. Signals were referenced to residual solvent signals. ^{31}P spectra are proton decoupled for clarity reasons. Elemental analyses were performed in the microanalytical laboratory of Technische Universität München.

DFT calculations

All calculations were performed with GAUSSIAN-09 [43] using the density functional/Hartree–Fock hybrid model Becke3LYP[44–46] and the split valence double-ζ (DZ) basis set 6-31+G**.[47–50] Re atoms were described with a Stuttgart 1997 ECP with a DZ description of the valence electrons.[51] No symmetry or internal coordinate constraints were applied during optimizations. All reported intermediates were verified as being true minima by the absence of negative eigenvalues in the vibrational frequency analysis. *XYZ* coordinates for all calculated compounds can be found in the ESI.†

Synthesis of *cis*-[Re(CO)$_3$Cl(η^1-C$_5$H$_4$ClP)$_2$] (1)

2-Chlorphosphinine (91.0 mg, 0.69 mmol, 2.50 eq.) was added to a suspension of [Re(CO)$_5$Cl] (100 mg, 0.28 mmol, 1.00 eq.) in 3 mL toluene in a Schlenk tube. The mixture was heated to reflux for 4 h. After some time the mixture turned yellow and the precursor dissolved gradually. After 4 h the solution was allowed to cool down to rt and toluene was removed *in vacuo* to afford a yellow solid. Analytically pure yellow crystals suitable for single crystal X-ray diffraction of **1** were obtained from CH_2Cl_2/pentane. (Yield 154 mg, 98%) ^{1}H NMR ($CDCl_3$): δ = 8.79 (ddd, $^2J_{H6-P}$ = 20.5 Hz, $^3J_{H6-H5}$ = 10.2 Hz, $^4J_{H6-H4}$ = 1.3 Hz, 2H), 8.00 (ddt, $^3J_{H3-H4}$ = 8.9 Hz, $^3J_{H3-P}$ = 13.6 Hz, $^3J_{H3-H6}$ = 1.0 Hz, 2H), 7.89 (dddd, $^3J_{H5-P}$ = 24.9 Hz, $^3J_{H5-H6}$ = 10.3 Hz, $^3J_{H5-H4}$ = 8.1 Hz, $^4J_{H5-H3}$ = 1.0 Hz, 2H), 7.47 (dd, $^3J_{H4-H5}$ = 7.9 Hz, $^4J_{H4-H6}$ = 1.3 Hz, 2H). ^{13}C NMR ($CDCl_3$): δ = 156.21 (dd, $^1J_{C-P}$ = 18.9 Hz, $^3J_{C-P}$ = 13.0 Hz, C_2), 146.93 (dd, $^1J_{C-P}$ = 15.0 Hz, $^3J_{C-P}$ = 10.5 Hz, C_6), 138.58 (t, $^3J_{C-P}$ = 5.3 Hz, C_4), 136.28 (d, $^2J_{C-P}$ = 9.5 Hz, C_5 or C_3), 129.78 (t, $^2J_{C-P}$ = 13.9 Hz, C_3 or C_5). ^{31}P NMR ($CDCl_3$): δ = 169.4. IR (ATR) ν [cm^{-1}]: 2046, 1992, 1945, 1699, 1652, 1558, 1540, 1506, 1394, 1352, 997, 858, 798, 739, 734, 598, 586, 573, 523, 505, 482, 442, 420. UV/vis (CH_2Cl_2): λ_{max} [nm] ($\varepsilon \times 10^3$ [L mol^{-1} cm^{-1}]) = 310 (6.3). Anal. calcd for $C_{13}H_8Cl_3O_3P_2Re$ (566.71): C, 27.55; H, 1.42. Found: C, 27.56; H, 1.39.

Synthesis of *mer*-[Re(CO)$_2$Cl(η^1-C$_5$H$_4$ClP)$_3$] (2)

Complex **1** (156 mg, 0.28 mmol, 1.00 eq.) and 2-chlorphosphinine (36.5 mg, 0.28 mmol, 1.00 eq.) were dissolved in 3 mL toluene in a Schlenk tube and refluxed for 4 h. After the solvent was removed *in vacuo*, crystallization from CH_2Cl_2/pentane afforded **1** as yellow crystals in addition to dark yellow crystals of **2**. (Yield 27.8 mg, 15%) ^{1}H NMR ($CDCl_3$): δ = 8.85 (dd, $^2J_{H6'-P}$ = 20.4 Hz, $^3J_{H6'-H5'}$ = 10.2 Hz, 1H), 8.57 (qd, $^3J_{H6-H5}$ = 10.1 Hz, $^4J_{H6-H4}$ = 1.3 Hz, 2H), 7.97 (q, $^3J_{H3-P}$ = 7.9 Hz, 2H), 7.84 (m, 4H), 7.37 (t, $^3J_{H4'-H5'}$ = 8.2 Hz, 1H), 7.31 (dt, $^3J_{H4-H5}$ = 7.4 Hz, $^4J_{H4-H6}$ = 3.5 Hz, 2H). ^{13}C NMR ($CDCl_3$): δ = 189.33 (dd, $^2J_{C-P}$ = 75 Hz, $^2J_{C-P}$ = 11 Hz, CO), 186.19 (m, CO), 156.21 (dt, $^1J_{C-P}$ = 26.2 Hz, J_{C-P} = 2.7 Hz, C_{ar}), 154.69 (td, $^1J_{C-P}$ = 18.3 Hz, J_{C-P} = 3.1 Hz, C_{ar}), 145.73 (m, C_{ar}), 138.39 (m, C_{ar}), 136.21 (t, J_{C-P} = 7.6 Hz, C_{ar}), 135.8 (d, $^1J_{C-P}$ = 16.9 Hz, C_{ar}), 128.74 (t, J_{C-P} = 24.3 Hz, C_{ar}), 127.7 (d, J_{C-P} = 12.7 Hz, C_{ar}). ^{31}P NMR ($CDCl_3$): δ = 173.1 (ps, 1P), 173.3 (pd, $^2J_{P-P\ tans}$ = 190 Hz, 2P). IR (ATR) ν [cm^{-1}]: 1965, 1924, 1628, 1292, 1265, 1182, 1138, 1130, 939, 910, 872, 864, 814, 731, 715, 669, 602, 582. UV/vis (CH_2Cl_2): λ_{max} [nm] ($\varepsilon \times 10^3$ [L mol^{-1} cm^{-1}]) = 394 (8.3), 335 (12.7). Anal. calcd for $C_{17}H_{12}Cl_4O_2P_3Re$ (669.22): C, 30.51; H, 1.81. Found: C, 30.27; H, 1.71.

Conflict of interest

The authors declare no competing financial interests.

Acknowledgements

M. H. is grateful for the financial support of the TUM Graduate School of Chemistry. M. H. thanks the Leibniz Rechenzentrum of the Bavarian Academy of Science for provision of computing time. Dr A. Pöthig's support with crystallographic data is greatly appreciated. S. M. gratefully acknowledges the Beilstein Institute for financial support.

Notes and references

1 P. Le Floch and F. Mathey, *Coord. Chem. Rev.*, 1998, **178**, 771.
2 P. Le Floch, *Coord. Chem. Rev.*, 2006, **250**, 627.
3 L. Kollár and G. Keglevich, *Chem. Rev.*, 2010, **110**, 4257.
4 C. Müller, L. E. E. Broeckx, I. de Krom and J. J. M. Weemers, *Eur. J. Inorg. Chem.*, 2013, **2013**, 187.
5 L. Nyulaszi and G. Keglevich, *Heteroat. Chem.*, 1994, **5**, 131.
6 F. Mathey and P. LeFloch, *Chem. Ber.*, 1996, **129**, 263.
7 A. J. Ashe, *Acc. Chem. Res.*, 1978, **11**, 153.
8 G. Märkl, *Angew. Chem., Int. Ed.*, 1966, **5**, 846.
9 P. Le Floch and F. Mathey, *Tetrahedron Lett.*, 1989, **30**, 817.
10 P. Le Floch, L. Ricard and F. Mathey, *Polyhedron*, 1990, **9**, 991.
11 P. Le Floch, D. Carmichael, L. Ricard and F. Mathey, *J. Am. Chem. Soc.*, 1993, **115**, 10665.
12 C. Elschenbroich, M. Nowotny, A. Behrendt, W. Massa and S. Wocadlo, *Angew. Chem., Int. Ed.*, 1992, **31**, 1343.
13 C. Elschenbroich, J. Six and K. Harms, *Chem. Commun.*, 2006, **32**, 3429.

14 P. Roesch, J. Nitsch, M. Lutz, J. Wiecko, A. Steffen and C. Müller, *Inorg. Chem.*, 2014, **53**, 9855.
15 L. E. E. Broeckx, W. Delaunay, C. Latouche, M. Lutz, A. Boucekkine, M. Hissler and C. Müller, *Inorg. Chem.*, 2013, **52**, 10738.
16 A. C. Carrasco, E. A. Pidko, A. M. Masdeu-Bulto, M. Lutz, A. L. Spek, D. Vogt and C. Muller, *New J. Chem.*, 2010, **34**, 1547.
17 C. Müller, E. A. Pidko, M. Lutz, A. L. Spek and D. Vogt, *Chem.–Eur. J.*, 2008, **14**, 8803.
18 T. Kojima, Y. Ishioka and Y. Matsuda, *Chem. Commun.*, 2004, **4**, 366.
19 B. Breit, R. Winde, T. Mackewitz, R. Paciello and K. Harms, *Chem.–Eur. J.*, 2001, **7**, 3106.
20 B. Breit, R. Winde and K. Harms, *J. Chem. Soc., Perkin Trans. 1*, 1997, 2681.
21 Y. Mao, K. M. H. Lim, Y. Li, R. Ganguly and F. Mathey, *Organometallics*, 2013, **32**, 3562.
22 J. Moussa, L. M. Chamoreau and H. Amouri, *RSC Adv.*, 2014, **4**, 11539.
23 N. Mézailles, F. Mathey and P. L. Floch, in *Prog. Inorg. Chem.*, John Wiley & Sons, Inc., 2001, pp. 455–550.
24 See ESI† for VT-NMR spectra.
25 S. Bucknor, F. A. Cotton, L. R. Falvello, A. H. Reid and C. D. Schmulbach, *Inorg. Chem.*, 1986, **25**, 1021.
26 H. D. Kaesz, R. Bau, D. Hendrickson and J. M. Smith, *J. Am. Chem. Soc.*, 1967, **89**, 2844.
27 C. Elschenbroich, J. Six, K. Harms, G. Frenking and G. Heydenrych, *Eur. J. Inorg. Chem.*, 2008, **2008**, 3303.
28 C. Elschenbroich, M. Nowotny, J. Kroker, A. Behrendt, W. Massa and S. Wocadlo, *J. Organomet. Chem.*, 1993, **459**, 157.
29 S. Erhardt and G. Frenking, *J. Organomet. Chem.*, 2009, **694**, 1091.
30 G. Albertin, S. Antoniutti, J. Castro, S. García-Fontán and G. Zanardo, *Organometallics*, 2007, **26**, 2918.
31 L. Salem and C. Rowland, *Angew. Chem., Int. Ed.*, 1972, **11**, 92.
32 J. P. Foster and F. Weinhold, *J. Am. Chem. Soc.*, 1980, **102**, 7211.
33 A. E. Reed and F. Weinhold, *J. Chem. Phys.*, 1983, **78**, 4066.
34 A. E. Reed and F. Weinhold, *J. Chem. Phys.*, 1985, **83**, 1736.
35 A. E. Reed, R. B. Weinstock and F. Weinhold, *J. Chem. Phys.*, 1985, **83**, 735.
36 A. E. Reed, L. A. Curtiss and F. Weinhold, *Chem. Rev.*, 1988, **88**, 899.
37 J. E. Carpenter and F. Weinhold, *J. Mol. Struct.: THEOCHEM*, 1988, **169**, 41.
38 F. Weinhold and J. Carpenter, in *The Structure of Small Molecules and Ions*, ed. R. Naaman and Z. Vager, Springer, US, 1988, ch. 24, pp. 227–236.
39 A. M. Kinnear and E. A. Perren, *J. Chem. Soc., Dalton Trans.*, 1952, 3437.
40 R. K. Harris, M. Lewellyn, M. I. M. Wazeer, J. R. Woplin, R. E. Dunmur, M. J. C. Hewson and R. Schmutzler, *J. Chem. Soc., Dalton Trans.*, 1975, **1**, 61.
41 K. Karaghiosoff, R. Mahnot, C. Cleve, N. Gandhi, R. K. Bansal and A. Schmidpeter, *Chem. Ber.*, 1995, **128**, 581.
42 E. Uhing, K. Rattenbury and A. D. F. Toy, *J. Am. Chem. Soc.*, 1961, **83**, 2299.
43 M. J. Frisch, G. W. Trucks, H. B. Schlegel, G. E. Scuseria, M. A. Robb, J. R. Cheeseman, G. Scalmani, V. Barone, B. Mennucci, G. A. Petersson, H. Nakatsuji, M. Caricato, X. Li, H. P. Hratchian, A. F. Izmaylov, J. Bloino, G. Zheng, J. L. Sonnenberg, M. Hada, M. Ehara, K. Toyota, R. Fukuda, J. Hasegawa, M. Ishida, T. Nakajima, Y. Honda, O. Kitao, H. Nakai, T. Vreven, J. A. Montgomery, J. E. P. Jr, F. Ogliaro, M. Bearpark, J. J. Heyd, E. Brothers, K. N. Kudin, V. N. Staroverov, R. Kobayashi, J. Normand, K. Raghavachari, A. Rendell, J. C. Burant, S. S. Iyengar, J. Tomasi, M. Cossi, N. Rega, J. M. Millam, M. Klene, J. E. Knox, J. B. Cross, V. Bakken, C. Adamo, J. Jaramillo, R. Gomperts, R. E. Stratmann, O. Yazyev, A. J. Austin, R. Cammi, C. Pomelli, J. W. Ochterski, R. L. Martin, K. Morokuma, V. G. Zakrzewski, G. A. Voth, P. Salvador, J. J. Dannenberg, S. Dapprich, A. D. Daniels, Ö. Farkas, J. B. Foresman, J. V. Ortiz, J. Cioslowski and D. J. Fox, *Gaussian 09, Revision D.01*, Gaussian Inc., Wallingford CT, 2009.
44 S. H. Vosko, L. Wilk and M. Nusair, *Can. J. Phys.*, 1980, **58**, 1200.
45 C. T. Lee, W. T. Yang and R. G. Parr, *Phys. Rev. B: Condens. Matter Mater. Phys.*, 1988, **37**, 785.
46 A. D. Becke, *J. Chem. Phys.*, 1993, **98**, 5648.
47 W. J. Hehre, R. Ditchfield and J. A. Pople, *J. Chem. Phys.*, 1972, **56**, 2257.
48 M. M. Francl, W. J. Pietro, W. J. Hehre, J. S. Binkley, M. S. Gordon, D. J. Defrees and J. A. Pople, *J. Chem. Phys.*, 1982, **77**, 3654.
49 T. Clark, J. Chandrasekhar, G. W. Spitznagel and P. V. R. Schleyer, *J. Comput. Chem.*, 1983, **4**, 294.
50 P. C. Hariharan and J. A. Pople, *Theor. Chim. Acta*, 1973, **28**, 213.
51 D. Andrae, U. Häußermann, M. Dolg, H. Stoll and H. Preuß, *Theor. Chim. Acta*, 1990, **77**, 123.